Effects of Orotic Acid-Induced Non-Alcoholic Fatty Liver on the Pharmacokinetics of Metoprolol and its Metabolites in Rats

Won Seok Bang[1,a], Ye Ran Hwang[1,a], Zhengri Li[1], Inchul Lee[2], Hee Eun Kang[1]

[1] College of Pharmacy and Integrated Research Institute of Pharmaceutical Sciences, The Catholic University of Korea, Bucheon, South Korea. [2] Department of Diagnostic Pathology, College of Medicine, University of Ulsan, Asan Foundation, Asan Medical Center, Seoul, South Korea.

ABSTRACT - Purpose: Preliminary study results have shown that rats with non-alcoholic fatty liver disease (NAFLD) induced by 1% orotic acid-containing diet have decreased hepatic CYP2D activity. This study aims to evaluate the possible pharmacokinetic changes in NAFLD as a result of reduced metabolic activity of CYP2D. **Methods:** The pharmacokinetics of metoprolol and its metabolites, *O*-desmethyl metoprolol (DMM) and α-hydroxy metoprolol (HM), was investigated in NAFLD and control rats following intravenous (1 mg/kg) and oral (2 mg/kg) administration of metoprolol. The hepatic CYP2D expression was also investigated. **Results:** NAFLD rats had lower CYP2D expression (by 36.6%) and slower intrinsic clearance (CL_{int}) of metoprolol and formation of HM (by 40.1% and 37.2%, respectively). There were no significant changes in the pharmacokinetics of metoprolol and its metabolites following intravenous administration. In contrast, oral administration of metoprolol resulted in significantly increased total area under plasma concentration-time curve (AUC) of metoprolol (by 127%) and decreased metabolite formation ratios ($AUC_{DMM}/AUC_{Metoprolol}$ [by 42.8%], $AUC_{HM}/AUC_{Metoprolol}$ [by 35.0%]) in NAFLD rats. Moreover, these changes were well correlated with severity of steatosis as quantified by hepatic triglyceride contents. **Conclusions:** NALFD can lead to a reduction in the hepatic CL_{int} of a drug if it is a substrate of the CYP2D subfamily. The decreased clearance may result in elevated drug concentrations and increased exposure.

INTRODUCTION

Non-alcoholic fatty liver disease (NAFLD) refers to a spectrum of liver diseases that range from simple fatty liver (steatosis) to more severe non-alcoholic steatohepatitis (NASH). NAFLD is clinically important because it has a high prevalence (25% of the general population) and a wide spectrum of histologic damage that can lead to NASH, cirrhosis, hepatocellular carcinoma, and liver failure (1). Obesity and obesity-related conditions (insulin resistance, dyslipidemia, and high blood pressure) have also been identified as predisposing conditions for NAFLD (2, 3).

Hepatic disease is regarded as a primary factor that can alter the disposition of many drugs (4). In fact, several published studies have documented changes in the cytochrome P450 (CYP) isozymes of NAFLD animal models. These changes include decreased expression and activity of hepatic CYP2C11, 3A2, 2A1/2, and 2B1 in microvesicular steatosis rats induced by orotic acid (OA) (5) or in NASH rats induced by methionine-choline deficient (MCD) diet (6); increased mRNA levels of CYP3A2, 2D2, and 2E1 in NASH rats (7); and controversial changes in CYP2E1 in NASH rats induced with OA diet or MCD diet (8, 9). Transcriptional, translational, and activity changes in hepatic CYP isozymes have also been reported in humans as NAFLD progresses (10). The variety of changes in hepatic CYP enzymes in animal models and patients with NAFLD suggest that possible pharmacokinetic changes of drugs may occur via several mechanisms as NAFLD progresses.

Corresponding Author: Hee Eun Kang; College of Pharmacy and Integrated Research Institute of Pharmaceutical Sciences, The Catholic University of Korea, San 43-1, Yeokgok 2-Dong, Wonmi-Gu, Bucheon 14662, South Korea; E-mail: kanghe@catholic.ac.kr. [a] **These two authors contributed equally to this work.**

Several therapeutically important agents are known to cause microvesicular steatosis. Therefore, evaluating the effects of lipid-mediated injury on hepatic drug metabolism is clinically significant. To evaluate possible pharmacokinetic changes in the early stages of NAFLD, a rat model of NAFLD induced by a diet containing 1% OA was used in this study (1, 11). OA is an intermediate metabolite in pyrimidine metabolism and produces rapid and extensive microvesicular steatosis in rats (5). The molecular mechanisms for the development of NAFLD in rats fed an OA diet have been reported (1, 11). Because OA is normally a minor component of diet (cow's milk, dairy products, and root vegetables), normal consumption of dietary OA is not expected to induce steatosis in human (12, 13). In our preliminary study, we compared the metabolism of various CYP probe substrates in hepatic microsomal fractions of rats with NAFLD induced by an OA diet with that of control rats. NAFLD rats exhibited significantly decreased dextromethorphan O-demethylase activity (by 31.4%), which represents the metabolic activity of rat CYP2D isoforms (14), when compared with that of controls (Figure 1). Moreover, in patients with NAFLD, hepatic microsomal protein expression of CYP2D6 tends to decrease with disease progression (10). The CYP2D isoforms from rats and humans have been reported to share a high sequence identity (>70%) (15). Therefore, evaluating possible pharmacokinetic changes in NAFLD due to reduced metabolic activity of CYP2D is considered a high priority.

Metoprolol, a selective β_1-adrenergic receptor antagonist, is widely used for the treatment of hypertension, angina pectoris, myocardial infarction, and arrhythmia (16). It also has a favorable effect on atherosclerosis development (17). In humans, around 75% of the metoprolol dose is metabolized hepatically by O-demethylation via CYP2D6 and unidentified CYP(s) (65% of the dose) and by α-hydroxylation (10% or less of the dose) via CYP2D6 (18). As metoprolol is also metabolized by the CYP2D subfamily in rats

(7, 19), metoprolol could be a clinically relevant model substrate for studying alterations in pharmacokinetics resulting from the reduced metabolic activity of CYP2D in NAFLD. Therefore, we examined the pharmacokinetics of metoprolol and its metabolites (*O*-desmethyl metoprolol and α-hydroxy metoprolol) in a well-established OA diet-induced NAFLD rat model after intravenous and oral administration of metoprolol.
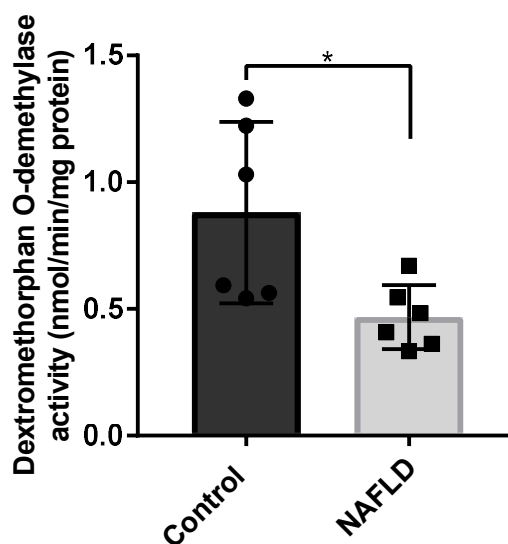
Figure 1. Dextromethorphan *O*-demethylase activity in hepatic microsomes of control and non-alcoholic fatty liver disease (NAFLD) rats. Individual hepatic microsomal fractions (0.5 mg protein) from control and NAFLD rats (n = 6 per group) were incubated with 100 μM dextromethorphan. $^*P$ < 0.05 compared to control values is considered statistically significant. Bars represent SD.

MATERIALS AND METHODS

Chemicals

Metoprolol tartrate, propranolol hydrochloride (internal standard [IS] for LC-MS/MS analysis of metoprolol, *O*-desmethyl metoprolol [DMM], and α-hydroxy metoprolol [HM]), dextrorphan, paracetamol (IS for LC-MS/MS analysis of dextrorphan), orotic acid monohydrate (OA), the reduced form of β-nicotinamide adenine dinucleotide phosphate (NADPH) as a tetrasodium salt, and Tris(hydroxymethyl)aminomethane (Tris)-buffer were all purchased from Sigma-Aldrich (St.

Louis, MO, USA). DMM, HM, and dextromethorphan were products from Santa Cruz Biotechnology (Santa Cruz, CA, USA). Other chemicals were of reagent or HPLC grade.

Animals and OA-induced NAFLD
All animal experiment protocols were approved by the Department of Laboratory Animals, Institutional Animal Care and Use Committee (IACUC) of Sungsim Campus, The Catholic University of Korea, Bucheon, South Korea. Male Sprague–Dawley rats (4–5 weeks old) were purchased from Young Bio (Seongnam, South Korea). The procedures used for housing and handling rats were similar to those described previously (20). After an adaption period of 3 days, rats were randomly divided into two groups. One group was given a normal purified rodent diet (AIN-93G) (control group) and the other group received an OA diet prepared by supplementing the normal diet with 1% w/w OA (NAFLD group). The dietary consumption of both groups was measured and animals were allowed free access to water. Animals were maintained for 20 days and underwent a fasting period of 15 h prior to experimentation.

Preliminary study
The following preliminary studies were performed in rats on day 21 after the start of feeding in control (control rats; $n = 6$) or OA diet (NAFLD rats; $n = 6$) groups to verify whether NAFLD was induced and to estimate liver and kidney functions. A urine sample was collected at 15 h to measure creatinine levels. Levels of albumin, urea nitrogen, aspartate aminotransferase (AST), alanine aminotransferase (ALT), and creatinine were also measured using plasma samples obtained at 15 h (VetTest®, IDEXX Laboratories, Westbrook, ME, USA). The whole liver and kidneys of each rat were excised, rinsed with 0.9% NaCl-injectable solution, blotted dry with tissue paper, and weighed. Small portions of the liver and kidney were fixed in 10% neutral phosphate-buffered formalin and then processed for routine histological examination by hematoxylin & eosin staining. Approximately 0.2 g of liver from each rat was also stored at –70°C until analysis of hepatic triglyceride content using ethanolic potassium hydroxide saponification followed by a glycerol assay according to reported methods (21).

The hepatic microsomes from control and NAFLD rats were prepared (22) and the protein contents were measured (23). For measurement of dextromethorphan O-demethylation activity, the above hepatic microsomes from each group (equivalent to 0.5 mg protein) were pre-incubated with 0.1 M potassium phosphate buffer (pH 7.4) and 5 µL of methanol containing dextromethorphan (final concentrations of 100 µM) in a thermomixer (Thermomixer 5436; Eppendorf, Hamburg, Germany) at 37 °C and 600 rpm. To initiate the reaction, NADPH (in 0.1 M potassium phosphate buffer of pH 7.4 to a final concentration of 1 mM) was added to a final volume of 500 µL. At 10 min after the start of the reaction, 25 µL was collected and transferred to an Eppendorf tube containing 75 µL of acetonitrile with 30 µM of paracetamol (IS), and vortex-mixed to terminate the reaction. After mixing and centrifugation (16,000 g, 5 min), the supernatant was collected and dextrorphan was analyzed using LC-MS/MS.

Immunoblot analysis of hepatic CYP2D
The hepatic microsomal protein fractions (40 µg) were mixed with NuPAGE® LDS sample buffer (Thermo Fisher Scientific, Waltham, MA, USA) and subjected to electrophoresis using a NuPAGE® 4–12% Bis-Tris gel, and then transferred to a polyvinylidene difluoride membrane. After blocking in Tris-buffered saline containing 0.1% v/v Tween-20 and 5% w/v fat-free milk powder, the membranes were incubated with rabbit anti-CYP2D antibodies at a 1:1,000 dilution (Abcam, Cambridge, UK) followed by anti-rabbit conjugated horseradish peroxidase (HRP) secondary antibodies (Santa Cruz Biotechnology, Santa Cruz, CA, USA). Signals were detected using SuperSignal™ West Dura Extended Duration Substrate (Thermo Fisher Scientific) and the Chemidoc XRS imager system (Bio-Rad, Hercules, CA, USA). The β-actin band was used as a loading control.

Kinetics for the disappearance of metoprolol and formation of DMM and HM in hepatic microsomal fractions
The following components were mixed: the hepatic microsomal fractions prepared from each group (equivalent to 0.5 mg protein); 0.1 M phosphate buffer (pH 7.4); and 5 µL of distilled water containing metoprolol (final metoprolol concentrations of 5, 10, 20, 50, 75, 100, 150, and 200 µM). Mixtures were pre-incubated for 5 min in a thermomixer (Thermomixer 5436; Eppendorf) at 37°C and 600 rpm. To initiate the reaction, 1 mM NADPH in 0.1 M phosphate buffer (pH 7.4) was added to a final volume of 500 µL. After 15 min of incubation, an aliquot of 25 µL was transferred to a microcentrifuge tube containing 20 µL 0.5 N

sodium hydroxide and 25 μL methanol containing propranolol (IS, 1 μg/mL). The aliquot was vortex-mixed to terminate the reaction. Next, the mixture was extracted with 1 mL of diethyl ether and treated according to the sample preparation procedure described below.

All of the above microsomal incubation conditions were within the linear range of reaction rate with the given microsomal protein content based on previous reports (24). The kinetic constants (K_m, apparent Michaelis–Menten constant; and V_{max}, maximum velocity) for the disappearance of metoprolol were obtained by fitting the data to Lineweaver-Burk plots using SigmaPlot 9.0 (Systat Software Inc., San Jose, CA, USA). The kinetic constants for the formation of DMM and HM from metoprolol were calculated using a non-linear regression method (25) using SigmaPlot 9.0 (Systat Software Inc.). The unweighted kinetic data was fitted to a single-site Michaelis–Menten equation. The intrinsic clearance (CL_{int}) for the disappearance of metoprolol and the formation of DMM and HM was calculated by dividing V_{max} by K_m.

Measurement of plasma protein binding of metoprolol, DMM, and HM
Plasma protein binding values of metoprolol and its metabolites in control and NAFLD rats ($n = 6$ per group) were determined using the ultrafiltration method (26). Metoprolol, DMM, and HM were spiked into each 500-μL plasma sample to produce a final concentration of 200, 20, and 50 ng/mL, respectively. After a 20-min incubation to equilibrium in a thermomixer at 37°C and 600 rpm, 25 μL of the plasma was sampled to measure the total metoprolol, DMM, and HM concentrations. Additionally, 400 μL of the plasma was collected into a Microcon® centrifugal filter device (30,000 NMWL Filter Unit; Merck Millipore Ltd, Cork, Ireland) for ultrafiltration. The plasma samples were centrifuged (2,000 g; 37°C) for 20 min and a 25-μL portion of the upper and lower layers was stored at –70°C until LC-MS/MS analysis of metoprolol, DMM, and HM. Plasma protein binding values of metoprolol have been reported to be constant at 14.5% in the concentration range of 0.1 to 100 μg/mL (19). Thus, 200 ng/mL of metoprolol was used for the plasma protein binding study. Concentrations of metabolites were determined based on plasma concentration after metoprolol administration.

Intravenous and oral administration of metoprolol
The procedures used for the pretreatment of rats, including cannulation of the jugular vein and the carotid artery were similar to those reported previously (20). The fasting blood glucose levels were measured using the Medisense Optium kit (Abbott Laboratories, Bedford, MA, USA) before the start of pharmacokinetic study.

Metoprolol has been reported to show linear pharmacokinetics in the dose range used in this study (27, 28). Metoprolol tartrate (dissolved in 0.9% NaCl-injectable solution) at a dose of 1 mg (2 mL)/kg as free-base metoprolol was manually infused over 1 min via the jugular vein in control ($n = 7$) and NAFLD rats ($n = 8$). Blood samples (approximately 60 μL) were collected via the carotid artery at 0 (control), 1 (end of infusion), 5, 15, 30, 45, 60, 75, 90, 120, 150, and 180 min after the start of intravenous infusion. Blood samples were immediately centrifuged and 25 μL of plasma was collected and stored at –70°C until LC-MS/MS analysis of metoprolol, DMM, and HM. The procedures used for preparation and handling of urine samples to calculate the percentage of the dose excreted in the urine for 24 h ($Ae_{0-24 h}$) were similar to the method described previously (20). To confirm that NAFLD was successfully induced, an additional 0.2 g of liver from each rat was stored at –70°C until analysis of hepatic triglyceride content (21).

Metoprolol tartrate (dissolved in the same vehicle as the intravenous study) at a dose of 2 mg (in 4 mL)/kg as free-base metoprolol was orally administered to control ($n = 5$) and NAFLD rats ($n = 6$) using gastric gavage. Blood samples were collected via the carotid artery at 0, 5, 10, 15, 20, 30, 45, 60, 90, 120, 150, and 180 min after oral administration of the drug. Other procedures for the oral study were similar to those described for the intravenous study.

LC-MS/MS analysis
The LC-MS/MS system consisted of an Agilent 6460 triple quadrupole with an Agilent 1260 LC system (Agilent, Waldbronn, Germany). Instrument control and data acquisition were performed using Agilent MassHunter Workstation software (Version B. 04. 01).

For the quantification of dextrorphan in hepatic microsomal incubation samples, 1 μL of the supernatant was injected directly onto a reversed-phase HPLC column (C_{18}; 75 mm, l. × 4.6 mm, i.d.; particle size, 3.5 μm). The mobile phase, 2 mM

ammonium acetate:acetonitrile [50:50 (v/v)], was run through the column at a flow rate of 0.3 mL/min. The eluent was monitored using a triple quadrupole tandem mass spectrometer equipped with an electrospray ionization (ESI) source and operated in positive ion mode. The instrument parameters were set as follows: gas temperature, 350°C; sheath gas temperature, 250°C; gas flow, 5 L/min; sheath gas flow, 11 L/min; nebulizer, 45 psi; and electrospray voltage, 3.5 kV. The fragmentor voltage was set at 155 V for dextrorphan and 95 V for IS. The collision energy for dextrorphan and IS was 32 and 15 eV, respectively. The precursor to product ion transitions for dextrorphan and IS were m/z 258 ([M+H]$^+$) → 157 and m/z 152 ([M+H]$^+$) → 110, respectively. The retention times of dextrorphan and IS were approximately 6.6 and 2.6 min, respectively. The calibration range of dextrorphan in hepatic microsome samples was 0.1-10 μM.

Concentrations of metoprolol, DMM, and HM in the samples were simultaneously determined using the LC-MS/MS method developed in our laboratory. In brief, 20 μL of 0.5 N NaOH and 25 μL of methanol containing 1 μg/mL of IS (propranolol) were added to 25 μL of each biological sample. Then, the mixture was extracted with 1 mL diethyl ether. After mixing and centrifugation (16,000 × g, 5 min), the supernatant was collected and evaporated under a gentle stream of nitrogen gas at 40°C. The residue was reconstituted with 75 μL of a 1:1 (v/v) mixture of distilled water and methanol and 1 μL was injected directly onto a same reversed-phase HPLC column as above. The mobile phase, 5 mM formic acid in water:acetonitrile [80:20 (v/v)], was run through the column at a flow rate of 0.4 mL/min. The eluent was monitored using a triple quadrupole tandem mass spectrometer equipped with ESI source in positive ion mode and the same instrument parameters as above. The fragmentor voltage was set at 117 V for metoprolol, 140 V for HM, and 130 V for both DMM and the IS. The collision energy for metoprolol and DMM was 20 eV, and that for HM and the IS was 16 eV and 17 eV, respectively. The precursor to product ion transitions for metoprolol, DMM, HM, and IS were m/z 268.3 ([M+H]$^+$) → 116.2, m/z 254 ([M+H]$^+$) → 116, m/z 284.2 ([M+H]$^+$) → 116.1, and m/z 260.1 ([M+H]$^+$) → 183.1, respectively. The retention times of metoprolol, DMM, HM, and the IS were approximately 2.4, 1.4, 1.4, and 4.8 min, respectively.

The calibration ranges of metoprolol, DMM, and HM in plasma samples were 0.8–10,000 ng/mL, 2.5–200 ng/mL, and 2.5–1000 ng/mL, respectively. The ranges in urine samples were 50–10,000 ng/mL, 50–5000 ng/mL, and 20–5000 ng/mL, respectively. The ranges in hepatic microsome samples were 0.5–200 μM, 0.25–10 μM, and 0.25–20 μM, respectively. The intra- and inter-day coefficients of variation (CVs) of the analysis on three consecutive days were below 15.9%, and the assay accuracies ranged from 86.2–112%.

Pharmacokinetic analysis
The total area under the plasma concentration by time curve from time zero to infinity (AUC) was calculated using the trapezoidal rule-extrapolation method (29). Standard methods (30) were used to calculate the following pharmacokinetic parameters by non-compartmental analysis (WinNonlin; Pharsight Corporation, Mountain View, CA, USA): the time-averaged total body, renal, and non-renal clearances (CL, CL$_R$, and CL$_{NR}$, respectively), terminal half-life, mean residence time (MRT), apparent steady-state volume of distribution (V_{ss}), and the extent of absolute oral bioavailability (F). The peak plasma concentration (C_{max}) and time to reach C_{max} (T_{max}) were read directly from the experimental data.

STATISTICAL ANALYSIS

Differences between the two means for unpaired data were analyzed using the Student's t-test, with the exception of T_{max} for which Mann-Whitney test was used, and $P < 0.05$ was considered statistically significant. Correlation analysis was performed between pharmacokinetic parameters and hepatic triglyceride contents using IBM SPSS Statistics version 23 (IBM Corp., Armonk, NY, USA). All data are presented as means ± standard deviation (SD) unless otherwise specified.

RESULTS

Preliminary study
Induction of NAFLD in rats that were fed an OA diet was confirmed by the elevated hepatic triglyceride contents and fatty changes observed in liver microscopy. In rats fed an OA diet (NAFLD rats), the hepatic triglyceride content was significantly increased (by 377%) compared to that of control rats (Table 1). Based on the results of liver microscopy (Figure 2), control rats showed normal to minimal fatty change. In contrast, all of

the NAFLD rats studied showed severe fatty changes of the liver. There were no significant microscopic findings in the kidneys of either control or NAFLD rats (data not shown). The creatinine clearance (CL_{CR}) values in NAFLD rats were also comparable to those in controls (Table 1).

Body weight, diet consumption, plasma chemistry data, and relative weights of liver and kidneys in control and NAFLD rats are also listed in Table 1 and compared with the reported values in normal rats (31, 32). There was significantly less body weight gain in NAFLD rats compared to control rats, whereas the daily diet consumption was similar between the two groups. Urea nitrogen in the plasma of both groups was comparable and within the range of reported values in normal rats. Although the albumin level in plasma was significantly lower in NAFLD rats than in controls, the value was within the range of the reported normal value. The mean plasma levels of AST and ALT in NAFLD rats were significantly higher than those in control rats by 322% and 207%, respectively, and outweighed the reported normal range. A significant increase in relative liver weight of 24.3% was also observed in NAFLD rats.

Protein expression of hepatic CYP2D in control and NAFLD rats

The protein expression levels of hepatic CYP2D in control and NAFLD rats are shown in Figure 3. NAFLD rats exhibited a significant decrease in protein expression of hepatic CYP2D (36.6%) compared with that in control rats.

V_{max}, K_m, and CL_{int} for the disappearance of metoprolol and formation of DMM and HM in hepatic microsomes from control and NAFLD rats

The Lineweaver-Burk plots for metoprolol clearance in hepatic microsomes of control and NAFLD rats are shown in Figure 4A. The CL_{int} value for the disappearance of metoprolol in hepatic microsomes of NAFLD rats was significantly slower by 40.1% in NAFLD rats compared with controls (Table 2).

Table 1 Diet consumption, plasma chemistry data, renal creatinine clearance (CL_{cr}), hepatic triglyceride content, and relative liver and kidney weight (mean ± SD) in control and NAFLD rats (For comparison, the values in normal rats from the literature are also listed.)

Parameter	Control (n = 6)			NAFLD (n = 6)			Normal rats
Initial body weight (g)	139	±	3.76	136	±	3.76	
Final body weight (g)	281	±	8.61	245	±	15.2[***]	
Average diet consumption (g/day)		19.7			18.3		
Plasma chemistry							
Albumin (g/dL)	3.18	±	0.194	2.82	±	0.214[*]	2.70–5.10 [a]
Urea nitrogen (mg/dL)	13.2	±	2.04	13.5	±	1.64	5.0–29.0 [a]
AST (IU/L)	58.8	±	16.0	248	±	162[*]	45.7–80.8 [a]
ALT (IU/L)	22.0	±	9.06	67.5	±	36.7[*]	17.5–30.2 [a]
CL_{cr} (mL/min/kg)	6.09	±	2.63	6.02	±	1.95	5.24 [b]
Hepatic triglyceride (mg/g liver)	30.6	±	7.51	146	±	41.2[***]	
Liver weight (% of body weight)	3.83	±	0.128	4.76	±	0.397[***]	4.00 [b]
Kidney weight (% of body weight)	0.923	±	0.0719	0.804	±	0.0460[**]	0.80 [b]

[a] Values from the literature (31)
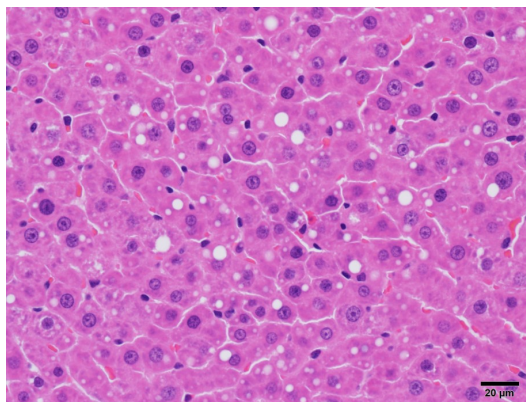[b] Calculated from the literature (32)
[*] Significantly different from the control group ([*]$P < 0.05$, [**]$P < 0.01$, [***]$P < 0.001$, t-test).
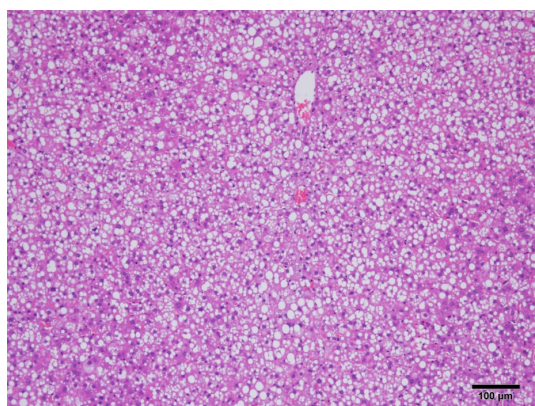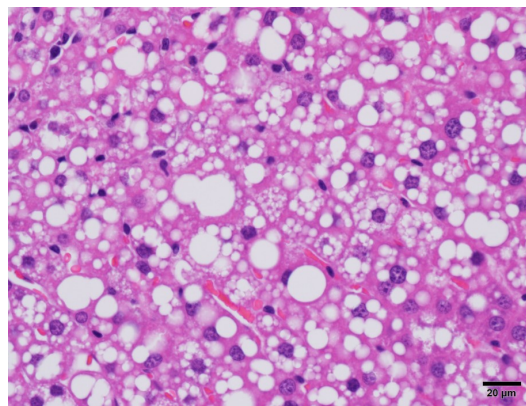
A-1
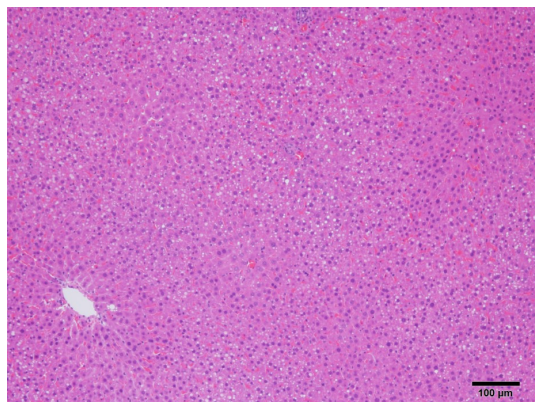
A-2

B-1

B-2

Figure 2. Liver histopathology of rats with and without NAFLD. Representative histopathology of liver sections from control (non-NAFLD) rats (A-1, 100× magnification; A-2, 400× magnification) and NAFLD rats (B-1, 100× magnification; B-2; 400× magnification). Liver sections were stained with hematoxylin and eosin prior to microscopy.

The mean velocities of DMM and HM formation from metoprolol in hepatic microsomes from control and NAFLD rats are shown in Figure 4B and 4C, respectively. In NAFLD rats, the V_{max} values for the formation of DMM and HM were both significantly slower by 45.7% and 53.4%, respectively, whereas the K_m values for the formation of the two metabolites were both lower by 42.6% and 27.3%, respectively, compared with those of the control group (Table 2). As a result, the CL_{int} values for the formation of DMM were comparable between the groups. However, the CL_{int} values for the formation of HM were significantly slower by 37.2% in NAFLD rats than in the control rats.

Plasma protein binding of metoprolol, DMM, and HM

The binding values of metoprolol to fresh rat plasma from control and NAFLD rats were comparable (7.41 ± 8.74% and 10.2 ± 7.92%, respectively). The binding values of DMM were also similar between the two groups (16.0 ± 3.51% and 16.9 ± 4.00%, respectively). Plasma protein binding of HM was negligible in both control and NAFLD rats. Non-specific binding of metoprolol, DMM, and HM to the centrifugal filter devices was negligible. There was a > 95.3% recovery of metoprolol, DMM, and HM after ultrafiltration was completed.
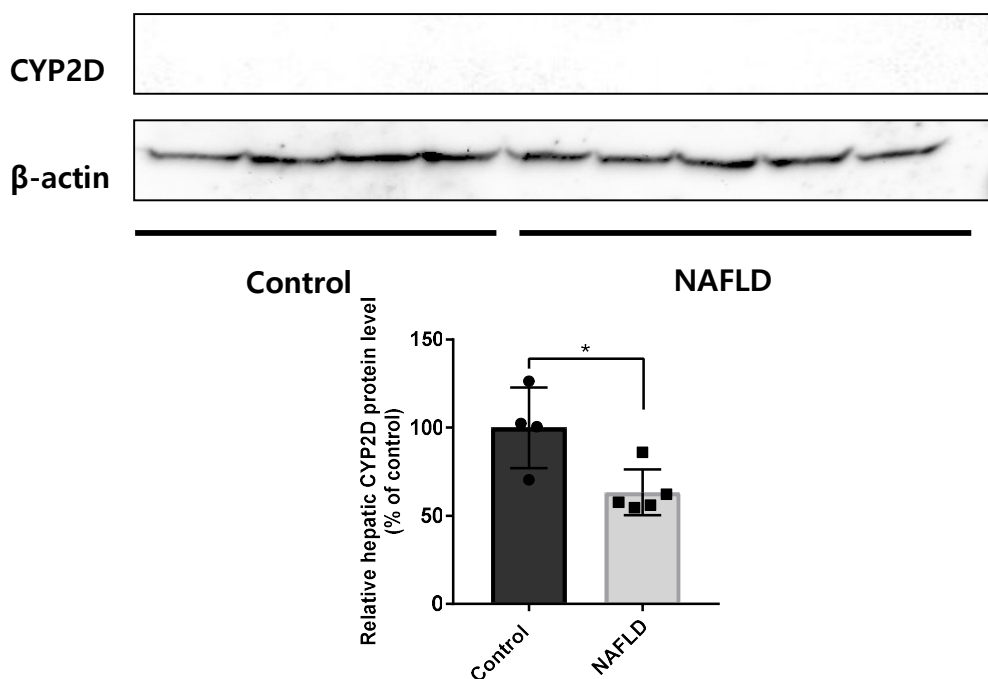
Figure 3. Expression of CYP2D in livers of rats with and without NAFLD. Immunoblots of hepatic CYP2D in control (non-NAFLD) and NAFLD rats (A) and relative expression levels (B). β-actin was used as a loading control. *$P < 0.05$ compared to control values is considered statistically significant. Bars represent SD.
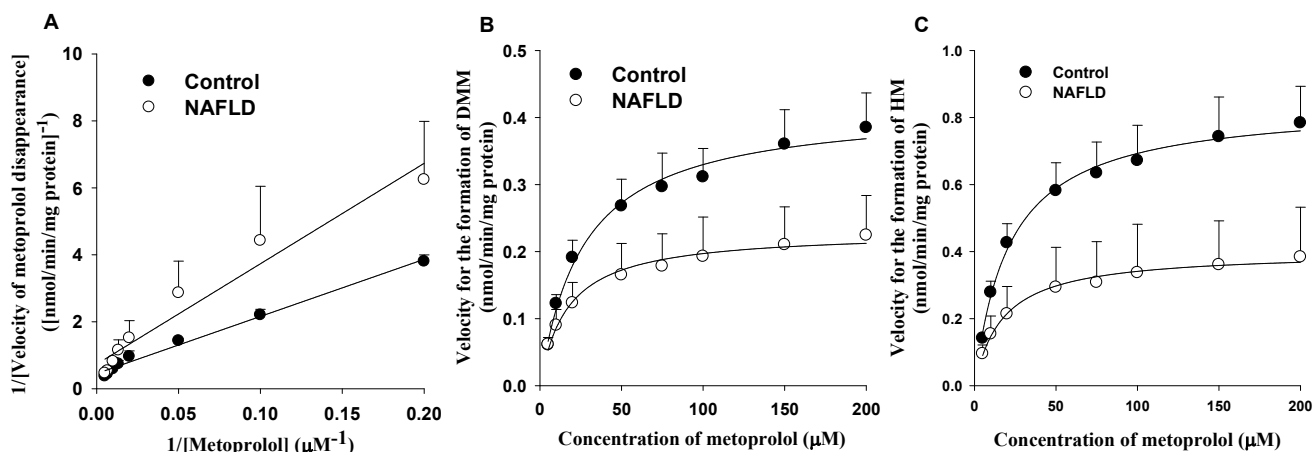
Figure 4. Metoprolol clearance and metabolite formation in rats with and without NAFLD. Lineweaver-Burk plot of the disappearance of metoprolol (A) and the mean velocities for formation of *O*-desmethyl metoprolol (DMM) (B) and α-hydroxy metoprolol (HM) (C) from various concentrations of metoprolol in hepatic microsomes of control (non-NAFLD) and NAFLD rats ($n = 6$ per group). Bars represent SD.

Pharmacokinetics of metoprolol, DMM, and HM after intravenous administration of metoprolol

The mean arterial plasma concentration–time profiles of metoprolol, DMM, and HM in control and NAFLD rats after intravenous administration of 1 mg/kg metoprolol are shown in Figure 5A–5C. The relevant pharmacokinetic parameters are listed in Table 3. Pharmacokinetic parameters of metoprolol were comparable between control and NAFLD rats. Additionally, the pharmacokinetic parameters of the two metabolites were also similar between the two groups with the exception of CL_R and C_{max}. The CL_R of DMM was significantly slower by 16.8% and the C_{max} of HM was significantly smaller by 30.1% in NAFLD rats than in controls.

Table 2 *In vitro* V_{max}, K_m, and CL_{int} values (mean ± SD) for the disappearance of metoprolol and the formation of DMM and HM in hepatic microsomal fractions from control and NAFLD rats.

Parameter	Control ($n = 6$)	NAFLD ($n = 6$)
Disappearance of metoprolol		
V_{max} (nmol/min/mg protein)	2.65 ± 0.462	2.07 ± 0.523
K_m (µM)	47.8 ± 9.90	67.2 ± 28.5
CL_{int} (µL/min/mg protein)	55.8 ± 3.26	33.4 ± 10.9[***]
Formation of DMM		
V_{max} (nmol/min/mg protein)	0.416 ± 0.0708	0.226 ± 0.0663[***]
K_m (µM)	26.3 ± 5.05	15.1 ± 2.78[***]
CL_{int} (µL/min/mg protein)	16.0 ± 2.10	14.9 ± 3.19
Formation of HM		
V_{max} (nmol/min/mg protein)	0.847 ± 0.145	0.395 ± 0.162[***]
K_m (µM)	22.0 ± 4.21	16.0 ± 2.37[*]
CL_{int} (µL/min/mg protein)	38.7 ± 4.37	24.3 ± 7.54[**]

[*] Significantly different from the control group ([*]$P < 0.05$, [**]$P < 0.01$, [***]$P < 0.001$, t-test).

Table 3 Pharmacokinetic parameters (mean ± SD) of metoprolol and its metabolites, DMM and HM, after intravenous administration of 1 mg/kg metoprolol to control and NAFLD rats.

| Parameter	Control ($n = 7$)	NAFLD ($n = 8$)
Initial body weight (g)	135 ± 7.07	134 ± 5.63
Final body weight (g)	272 ± 16.3	250 ± 21.7[*]
Liver weight (% of body weight)	3.46 ± 0.274	4.08 ± 0.241[***]
Hepatic Triglyceride (mg/g liver)	14.8 ± 2.55	153 ± 58.8[***]
Average diet consumption (g/day)	19.3	20.2
Fasting blood glucose (mg/dL)	108 ± 15.5	140 ± 22.8[**]
Metoprolol		
AUC (µg·min/mL)	10.1 ± 1.32	11.3 ± 2.15
Terminal half-life (min)	30.7 ± 3.21	32.2 ± 5.78
MRT (min)	20.2 ± 2.13	20.9 ± 5.65
CL (mL/min/kg)	100 ± 13.3	90.7 ± 13.5
CL_R (mL/min/kg)	22.8 ± 3.70	18.5 ± 4.23
CL_{NR} (mL/min/kg)	77.6 ± 11.4	72.2 ± 12.8
V_{ss} (mL/kg)	2050 ± 480	1930 ± 608
$Ae_{0-24 h}$ (% of metoprolol dose)	22.8 ± 2.67	20.6 ± 4.57
DMM		
AUC (µg·min/mL)	2.83 ± 0.316	3.89 ± 1.41
Terminal half-life (min)	62.7 ± 9.65	75.6 ± 16.1
C_{max} (ng/mL)	21.7 ± 2.47	25.4 ± 6.44
T_{max} (min) [a]	15 (5–30)	30 (18.8–45)
CL_R (mL/min/kg)	31.6 ± 3.09	26.3 ± 5.53[*]
$Ae_{0-24 h}$ (% of metoprolol dose)	9.37 ± 0.822	10.6 ± 4.01
$AUC_{DMM}/AUC_{Metoprolol}$ ratio	0.282 ± 0.0332	0.352 ± 0.128
HM		
AUC (µg·min/mL)	2.96 ± 0.673	2.86 ± 1.07
Terminal half-life (min)	50.8 ± 5.15	60.5 ± 13.3
C_{max} (ng/mL)	63.2 ± 13.2	44.2 ± 8.40[**]
T_{max} (min) [a]	5 (5)	5 (5–12.5)
CL_R (mL/min/kg)	46.3 ± 5.88	43.8 ± 15.3
$Ae_{0-24 h}$ (% of metoprolol dose)	12.8 ± 2.70	11.1 ± 3.72
$AUC_{HM}/AUC_{Metoprolol}$ ratio	0.294 ± 0.0609	0.258 ± 0.105

[a] Median (interquartile range)
[*] Significantly different from the control group ([*]$P < 0.05$, [**]$P < 0.01$, [***]$P < 0.001$, t-test).

Pharmacokinetics of metoprolol, DMM, and HM after oral administration of metoprolol
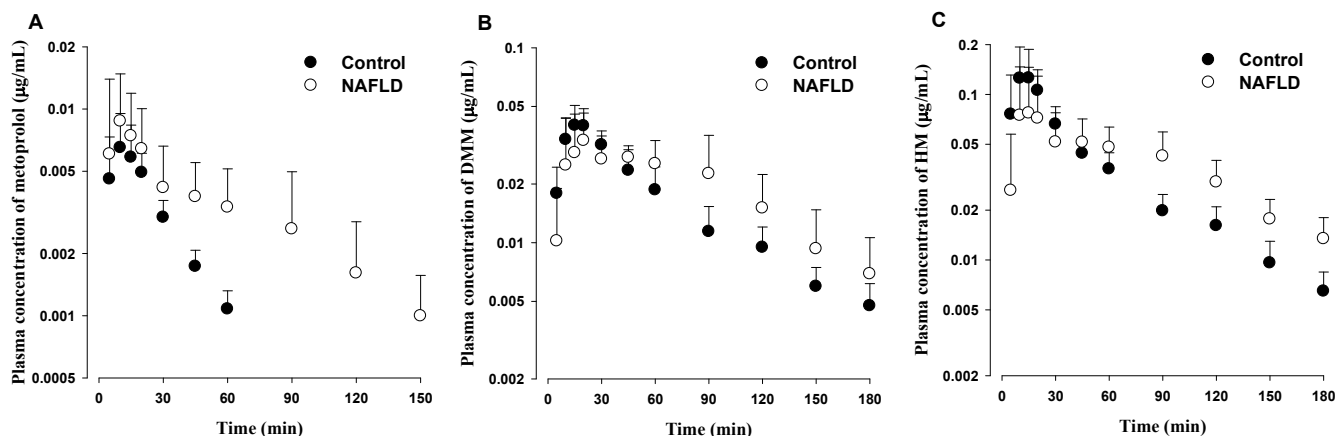
The mean arterial plasma concentration–time profiles of metoprolol, DMM, and HM after oral administration of 2 mg/kg metoprolol in control and NAFLD rats are shown in Figure 6A–6C. The relevant pharmacokinetic parameters are listed in Table 4. NAFLD rats showed the following changes in the pharmacokinetic parameters of metoprolol compared with controls: significantly greater AUC (by 127%); longer terminal half-life (by 56.7%); and greater $Ae_{0-24\ h}$ (by 136%). NAFLD rats also exhibited significantly or considerably smaller formation ratios of metabolites, $AUC_{DMM}/AUC_{Metoprolol}$ ratio (by 42.8%), and $AUC_{HM}/AUC_{Metoprolol}$ ratio (by 35.0%, $P = 0.0638$), compared to controls. Other pharmacokinetic parameters of DMM and HM including their AUCs were similar between control and NAFLD rats.
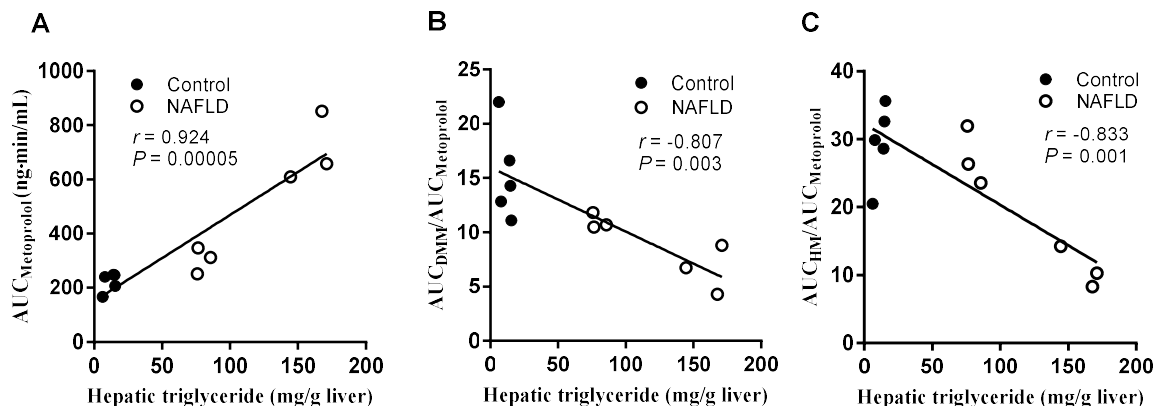
Based on correlation analysis, the AUC of metoprolol was positively correlated with hepatic triglyceride level (Pearson correlation coefficient, $r = 0.924$; $P < 0.001$). Both $AUC_{DMM}/AUC_{Metoprolol}$ ratio ($r = -0.807$; $P < 0.01$) and $AUC_{HM}/AUC_{Metoprolol}$ ratio ($r = -0.833$; $P < 0.01$) were negatively correlated with hepatic triglyceride level. The relationship of these pharmacokinetic parameters with hepatic triglyceride contents are shown in Figure 7.
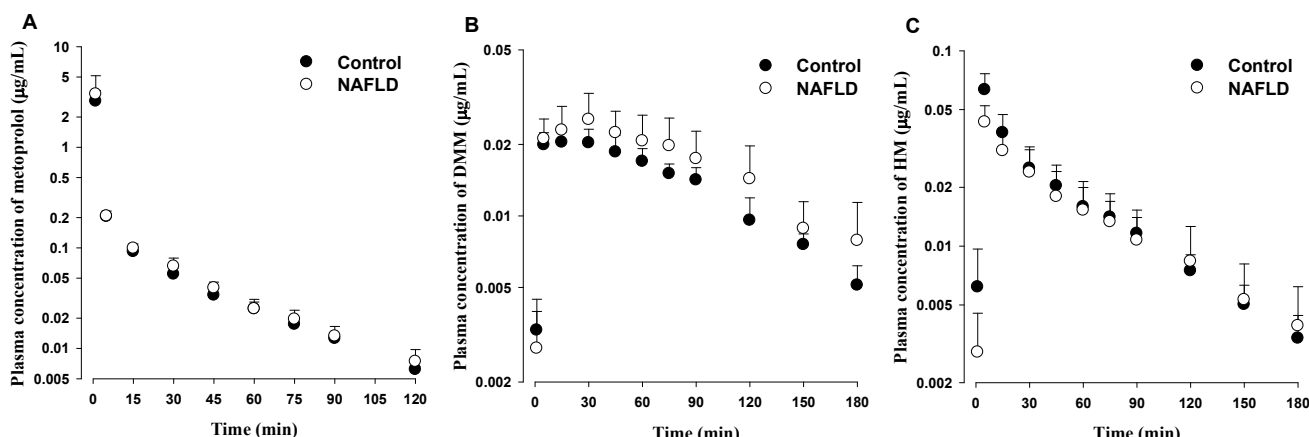
Figure 5. Mean arterial plasma concentration–time profiles of metoprolol and its metabolites following intravenous administration. Mean arterial plasma concentration–time profiles of metoprolol (A), DMM (B), and HM (C) after a single intravenous administration of 1 mg/kg metoprolol to control ($n = 7$) and NAFLD ($n = 8$) rats. Bars represent SD.

Figure 6. Mean arterial plasma concentration–time profiles of metoprolol and its metabolites following oral administration. Mean arterial plasma concentration–time profiles of metoprolol (A), DMM (B), and HM (C) after a single oral administration of 2 mg/kg metoprolol to control ($n = 5$) and NAFLD ($n = 6$) rats. Bars represent SD.

Figure 7. Pearson correlation analysis between hepatic triglyceride contents and pharmacokinetic parameters of oral metoprolol and its metabolites in NAFLD and control rats. The $AUC_{Metoprolol}$ following oral administration of metoprolol (A) is positively correlated with the hepatic triglyceride level ($r = 0.924$, $P = 0.00005$). $AUC_{DMM}/AUC_{Metoprolol}$ ($r = -0.807$, $P = 0.003$) (B) and $AUC_{HM}/AUC_{Metoprolol}$ ($r = -0.833$, $P = 0.001$) (C) ratios are negatively correlated with the hepatic triglyceride level.

Table 4 Pharmacokinetic parameters (mean ± SD) of metoprolol and its metabolites, DMM and HM, after oral administration of 2 mg/kg metoprolol to control and NAFLD rats.

Parameter	Control ($n = 5$)			NAFLD ($n = 6$)		
Initial body weight (g)	135	±	6.12	133	±	6.12
Final body weight (g)	270	±	7.91	218	±	9.35[***]
Liver weight (% of body weight)	4.47	±	0.292	5.60	±	0.520[**]
Hepatic Triglyceride (mg/g liver)	11.8	±	4.31	120	±	45.8[***]
Average diet consumption (g/day)		19.3			17.2	
Fasting blood glucose (mg/dL)	113	±	23.4	146	±	26.0
Metoprolol						
$\quad$ AUC (µg·min/mL)	0.222	±	0.0351	0.505	±	0.237[*]
$\quad$ Terminal half-life (min)	20.1	±	1.25	31.5	±	7.71[**]
$\quad$ C_{max} (ng/mL)	7.30	±	1.94	10.3	±	6.63
$\quad$ T_{max} (min) [a]		15 (10–17.5)			10 (8.75–22.5)	
$\quad$ CL_R (mL/min/kg)	26.9	±	6.25	27.9	±	5.99
$\quad$ Ae_{0-24h} (% of metoprolol dose)	0.295	±	0.0732	0.696	±	0.388[*]
$\quad$ F (%)		1.10			2.17	
DMM						
$\quad$ AUC (µg·min/mL)	3.34	±	0.691	3.92	±	0.992
$\quad$ Terminal half-life (min)	77.8	±	38.6	55.4	±	12.0
$\quad$ C_{max} (ng/mL)	44.7	±	4.55	40.3	±	12.4
$\quad$ T_{max} (min) [a]		15 (15–25)			60 (17.5–90)	
$\quad$ CL_R (mL/min/kg)	27.7	±	7.05	30.5	±	7.92
$\quad$ Ae_{0-24h} (% of metoprolol dose)	4.87	±	1.61	6.18	±	1.60
$\quad$ $AUC_{DMM}/AUC_{Metoprolol}$ ratio	15.4	±	4.21	8.81	±	2.83[*]
HM						
$\quad$ AUC (µg·min/mL)	6.63	±	1.83	7.84	±	0.946
$\quad$ Terminal half-life (min)	54.4	±	11.4	55.9	±	11.3
$\quad$ C_{max} (ng/mL)	141	±	57.8	101	±	64.5
$\quad$ T_{max} (min) [a]		15 (10–17.5)			60 (13.8–90)	
$\quad$ CL_R (mL/min/kg)	40.2	±	12.1	39.9	±	8.07
$\quad$ Ae_{0-24h} (% of metoprolol dose)	12.1	±	4.04	14.9	±	4.29
$\quad$ $AUC_{HM}/AUC_{Metoprolol}$ ratio	29.4	±	5.68	19.1	±	9.55

[a] Median (interquartile range)
[*] Significantly different from the control group ([*]$P < 0.05$, [**]$P < 0.01$, [***]$P < 0.001$, t-test).

DISCUSSION

An NAFLD rat model induced by a diet containing 1% OA was used in this study to evaluate possible pharmacokinetic changes of metoprolol in the early stages of NAFLD (1, 11). The results of a preliminary study indicated that NAFLD was successfully induced following an OA diet, with no significant kidney toxicities (Table 1 and Figure 2). Note that NAFLD rats also showed a mild elevation in fasting blood glucose levels (Tables 3 and 4), suggesting that this model resembles the clinical features of NAFLD, such as insulin resistance and hyperglycemia (33).

In the livers of NAFLD rats, there were significant decreases in protein expression of the CYP2D subfamily, consistent with our preliminary results showing a significant decrease in dextromethorphan O-demethylase (CYP2D) activity. Moreover, these decreases in expression and activity of CYP2D resulted in significantly slower *in vitro* hepatic CL_{int} values for the disappearance of metoprolol (40.1%) and formation of HM (37.2%) in NAFLD rats. It is important to note that a similar downregulation and decrease in activity of hepatic CYP2D6 in NAFLD patients with increasing disease severity has also been reported (10).

The AUC of intravenous metoprolol in NAFLD rats was similar to that in controls due to comparable metoprolol CL (Table 3). The AUC values of major metoprolol metabolites (DMM and HM) and their formation ratios ($AUC_{DMM}/AUC_{Metoprolol}$ and $AUC_{HM}/AUC_{Metoprolol}$) were also comparable between control and NAFLD rats. The major elimination pathway of metoprolol is hepatic metabolism (24, 27). Accordingly, the similar metoprolol CL and CL_{NR} of NAFLD rats and control rats suggests a similar hepatic metabolic clearance of metoprolol. Hepatic clearance of metoprolol primarily depends on its hepatic intrinsic clearance (CL_{int}), free fraction in plasma, and hepatic blood flow rate (34). The binding of metoprolol to plasma protein was comparable between control and NAFLD rats. However, there was no significant decrease in hepatic metoprolol CL despite a slower *in vitro* hepatic CL_{int} due to suppressed CYP2D activity in NAFLD rats. Because of the relatively high hepatic extraction ratio of metoprolol in rats [0.586–0.617 (27) or 0.84 by in situ-perfused rat liver (IPRL) (7)], it appears that hepatic blood flow significantly influences hepatic CL of metoprolol. For example, increased hepatic blood flow rate resulted in a faster hepatic CL of metoprolol measured in a diabetes rat model (24). Although reduced hepatic blood flow and microcirculation in fatty liver has been reported (35, 36), the present NAFLD rat model is in an early stage of fatty liver and appears to have normal hepatic blood flow rate.

While no significant pharmacokinetic changes in metoprolol and its metabolites were observed after intravenous administration, significantly increased AUC of metoprolol and decreased $AUC_{DMM}/AUC_{Metoprolol}$ and $AUC_{HM}/AUC_{Metoprolol}$ ratios were observed in NAFLD rats after oral administration of metoprolol (Table 4). Moreover, these changes were well correlated with the severity of the steatosis, which could be quantified by hepatic triglyceride contents (Figure 7). Based on significant reduction of *in vitro* CL_{int} of metoprolol by 40% in NAFLD rats, decrease of hepatic extraction ratio of metoprolol could be expected, although magnitude of the change could not quantitatively estimated primarily due to unknown hepatic blood flow in each group. Therefore, the greater oral AUC of metoprolol and smaller metabolite formation ratios ($AUC_{DMM}/AUC_{Metoprolol}$ and $AUC_{HM}/AUC_{Metoprolol}$ ratios) in NAFLD rats were primarily due to decreased hepatic first pass metabolism of metoprolol as a result of slowed hepatic CL_{int}, as shown by the comparable systemic CL values between NAFLD and control rats in the intravenous study. The decreased hepatic first pass metabolism of metoprolol in NAFLD rats is also supported by a previous study reporting a reduction in the hepatic extraction ratio of metoprolol in NASH compared to control (0.72 vs. 0.84) IPRLs (7). Faster CL_{int} of metoprolol in NASH than in control (1.8 vs. 1.13 mL/min/kg), which is opposite to our observation, was predicted in that study (7) by model fitting of perfusate concentrations. However, increase of CL_{int} of metoprolol in NASH is not likely to occur based on a study in human reporting a lower protein expression of CYP2D6 with progression of NAFLD (10) as well as our direct experimental observation (Figure 4, Table 2).

Because metoprolol reduces cardiac output and hepatic blood flow (37), higher metoprolol concentrations in NAFLD rats following its oral administration could possibly result in further decrease of hepatic CL of metoprolol. Considering that gastrointestinal absorption of metoprolol in rats is complete (27), it is not likely that the increased oral AUC of metoprolol in NAFLD rats is due to increased gastrointestinal absorption. However, possible alteration of gastrointestinal metabolism in

NAFLD rats could not be ruled out based on our results.

When a drug that is eliminated mainly by the liver is administered orally, systemic AUC is inversely proportional to hepatic CL_{int} (38). Therefore, rats with higher hepatic triglyceride contents might have slower hepatic CL_{int} and greater oral AUC of metoprolol. In NAFLD rats, the AUC values of metabolites following oral administration of metoprolol were not significantly different from those of controls, because increased oral AUC of metoprolol is a result of its decreased first pass effect.

CONCLUSION

NAFLD resulted in a slower hepatic CL_{int} of metoprolol and its decreased first pass metabolism as a result of reduced expression and activity of hepatic CYP2D. Consequently, NAFLD rats showed a significant increase in the AUC of metoprolol and a decrease in $AUC_{DMM}/AUC_{Metoprolol}$ and $AUC_{HM}/AUC_{Metoprolol}$ ratios following oral administration. Moreover, the magnitudes of these pharmacokinetic changes were well correlated with the severity of NAFLD. Considering that CYP2D isoforms are involved in the biotransformation of 30% of drugs on the market, this study underscores the need for further investigation of the pharmacokinetic changes related to the CYP2D enzyme subfamily in NAFLD patients. Caution is warranted when considering pharmacotherapy with drugs that are substrates of the CYP2D subfamily in NAFLD patients.

CONFLICT OF INTEREST

The authors declare no competing financial interests.

ACKNOWLEDGEMENTS

REFERENCES

1. Wang YM, Hu XQ, Xue Y, Li ZJ, Yanagita T, Xue CH. Study on possible mechanism of orotic acid-induced fatty liver in rats. Nutrition 2011; 27: 571-575.
2. Huang HL, Lin WY, Lee LT, Wang HH, Lee WJ, Huang KC. Metabolic syndrome is related to nonalcoholic steatohepatitis in severely obese subjects. Obes Surg 2007; 17: 1457-1463.
3. Targher G, Bertolini L, Rodella S, Zoppini G, Lippi G, Day C, et al. Non-alcoholic fatty liver disease is independently associated with an increased prevalence of chronic kidney disease and proliferative/laser-treated retinopathy in type 2 diabetic patients. Diabetologia 2008; 51: 444-450.
4. Lucena MI, Andrade RJ, Tognoni G, Hidalgo R, Sanchez de la Cuesta, F, Spanish Collaborative Study Group on Therapeutic Management of Liver Diseases. Drug use for non-hepatic associated conditions in patients with liver cirrhosis. Eur J Clin Pharmacol 2003; 59: 71-76.
5. Su GM, Sefton RM, Murray M. Down-regulation of rat hepatic microsomal cytochromes P-450 in microvesicular steatosis induced by orotic acid. J Pharmacol Exp Ther 1999; 291: 953-959.
6. Cho SJ, Kim SB, Cho HJ, Chong S, Chung SJ, Kang IM, et al. Effects of Nonalcoholic Fatty Liver Disease on Hepatic CYP2B1 and in Vivo Bupropion Disposition in Rats Fed a High-Fat or Methionine/Choline-Deficient Diet. J Agric Food Chem 2016; 64: 5598-5606.
7. Li P, Robertson TA, Thorling CA, Zhang Q, Fletcher LM, Crawford DH, et al. Hepatic pharmacokinetics of cationic drugs in a high-fat emulsion-induced rat model of nonalcoholic steatohepatitis. Drug Metab Dispos 2011; 39: 571-579.
8. Starkel P, Sempoux C, Leclercq I, Herin M, Deby C, Desager JP, et al. Oxidative stress, KLF6 and transforming growth factor-beta up-regulation differentiate non-alcoholic steatohepatitis progressing to fibrosis from uncomplicated steatosis in rats. J Hepatol 2003 ;39: 538-546.
9. Weltman MD, Farrell GC, Hall P, Ingelman-Sundberg M, Liddle C. Hepatic cytochrome P450 2E1 is increased in patients with nonalcoholic steatohepatitis. Hepatology 1998; 27: 128-133.
10. Fisher CD, Lickteig AJ, Augustine LM, Ranger-Moore J, Jackson JP, Ferguson SS, et al. Hepatic cytochrome P450 enzyme alterations in humans with progressive stages of nonalcoholic fatty liver disease. Drug Metab Dispos 2009; 37: 2087-2094.
11. Jung EJ, Kwon SW, Jung BH, Oh SH, Lee BH. Role of the AMPK/SREBP-1 pathway in the development of orotic acid-induced fatty liver. J Lipid Res 2011; 52: 1617-1625.
12. Salerno C, Crifò C. Diagnostic value of urinary orotic acid levels: applicable separation methods. J Chromatogr B Analyt Technol Biomed Life Sci 2002; 781: 57-71.
13. Löffler M, Carrey EA, Zameitat E. Orotic Acid, more than just an intermediate of pyrimidine de

novo synthesis. J Genet Genomics 2015; 42: 207-219.

14. Dostalek M, Hadasova E, Hanesova M, Pistovcakova J, Sulcova A, Jurica J, et al. Effect of methamphetamine on the pharmacokinetics of dextromethorphan and midazolam in rats. Eur J Drug Metab Pharmacokinet 2005; 30: 195-201.

15. Venhorst J, ter Laak AM, Commandeur JN, Funae Y, Hiroi T, Vermeulen NP. Homology modeling of rat and human cytochrome P450 2D (CYP2D) isoforms and computational rationalization of experimental ligand-binding specificities. J Med Chem 2003; 46: 74-86.

16. Ha HR, Follath F. Metabolism of antiarrhythmics. Curr Drug Metab 2004; 5: 543-571.

17. Hedblad B, Wikstrand J, Janzon L, Wedel H, Berglund G. Low-dose metoprolol CR/XL and fluvastatin slow progression of carotid intima-media thickness: Main results from the Beta-Blocker Cholesterol-Lowering Asymptomatic Plaque Study (BCAPS). Circulation 2001; 103: 1721-1726.

18. Lennard MS, Chapter 25. □-Adrenoceptor antagonists. In: Levy, R.H., Thummel, K.E., Trager, W.F., Hansten, P.D., Eichelbaum, M. (Eds.), Metabolite Drug Interaction. Philadelphia: Lippincott Williams & Wilkins, A Wolters Kluwer Company, 2000; p. 348.

19. Han SY, Yoon I, Chin YW, Cho IW, Lee MG, Choi YH. Pharmacokinetic interaction between metoprolol and SP-8203 in rats: competitive inhibition for the metabolism of metoprolol by SP-8203 via hepatic CYP2D subfamily. Xenobiotica 2012; 42: 1017-1027.

20. Lee YS, Kim YW, Kim SG, Lee I, Lee MG, Kang HE. Effects of poloxamer 407-induced hyperlipidemia on the pharmacokinetics of carbamazepine and its 10,11-epoxide metabolite in rats: Impact of decreased expression of both CYP3A1/2 and microsomal epoxide hydrolase. Eur Neuropsychopharmacol 2012; 22: 431-440.

21. Norris AW, Chen L, Fisher SJ, Szanto I, Ristow M, Jozsi AC, et al. Muscle-specific PPARgamma-deficient mice develop increased adiposity and insulin resistance but respond to thiazolidinediones. J Clin Invest 2003; 112: 608-618.

22. Lee JH, Lee MG. Telithromycin pharmacokinetics in rat model of diabetes mellitus induced by alloxan or streptozotocin. Pharm Res 2008; 25: 1915-1924.

23. Bradford MM. A rapid and sensitive method for the quantitation of microgram quantities of protein utilizing the principle of protein-dye binding. Anal Biochem 1976; 72: 248-254.

24. Lee U, Lee I, Lee BK, Kang HE. Faster non-renal clearance of metoprolol in streptozotocin-induced diabetes mellitus rats. Eur J Pharm Sci 2013; 50: 447-53.

25. Duggleby RG. Analysis of enzyme progress curves by nonlinear regression. Methods Enzymol 1995; 249: 61-90.

26. Kwon MH, Yoon JN, Baek YJ, Kim YC, Cho YY, Kang HE. Effects of poloxamer 407-induced hyperlipidemia on hepatic multidrug resistance protein 2 (Mrp2/Abcc2) and the pharmacokinetics of mycophenolic acid in rats. Biopharm Drug Dispos 2016; 37: 352-365.

27. Yoon IS, Choi MK, Kim JS, Shim CK, Chung SJ, Kim DD. Pharmacokinetics and first-pass elimination of metoprolol in rats: contribution of intestinal first-pass extraction to low bioavailability of metoprolol. Xenobiotica 2011; 41: 243-251.

28. Di Verniero CA, Silberman EA, Mayer MA, Opezzo JA, Taira CA, Hocht C. In vitro and in vivo pharmacodynamic properties of metoprolol in fructose-fed hypertensive rats. J Cardiovasc Pharmacol 2008; 51: 532-541.

29. Chiou WL. Critical evaluation of the potential error in pharmacokinetic studies of using the linear trapezoidal rule method for the calculation of the area under the plasma level--time curve. J Pharmacokinet Biopharm 1978; 6: 539-546.

30. Gibaldi M, Perrier D, Pharmacokinetics, second ed. New York: Marcel-Dekker, 1982.

31. Mitruka BM, Rawnsley HM. Clinical Biomedical and Hematological Reference Values in Normal Experimental Animals and Normal Humans, second ed. New York: Masson Publishing USA Inc., 1981.

32. Davies B, Morris T. Physiological parameters in laboratory animals and humans. Pharm Res 1993; 10: 1093-1095.

33. Marchesini G, Brizi M, Morselli-Labate AM, Bianchi G, Bugianesi E, McCullough AJ, et al. Association of nonalcoholic fatty liver disease with insulin resistance. Am J Med 1999; 107: 450-455.

34. Wilkinson GR, Shand DG. Commentary: a physiological approach to hepatic drug clearance. Clin Pharmacol Ther 1975; 18: 377-390.

35. Ijaz S, Yang W, Winslet MC, Seifalian AM. Impairment of hepatic microcirculation in fatty liver. Microcirculation 2003; 10: 447-456.

36. Farrell GC, Teoh NC, McCuskey RS. Hepatic microcirculation in fatty liver disease. Anat Rec (Hoboken) 2008; 291: 684-692.

37. Bauer LA, Horn JR, Maxon MS, Easterling TR, Shen DD, Strandness DE Jr. Effect of metoprolol and verapamil administered separately and concurrently after single doses on liver blood flow and drug disposition. J Clin Pharmacol 2000; 40: 533-543.

38. Benet LZ, Hoener BA. Changes in plasma protein binding have little clinical relevance. Clin Pharmacol Ther 2002; 71: 115-121.